

Table IV. Selected Bond Distances and Bond Angles for  $\text{Rh}_2\text{Cl}_2(\text{Ph}_2\text{P}(\text{C}_6\text{H}_4))_2(\text{PPh}_3)_2^a$ 

Bond Distances (Å)					
Rh-Rh'	2.499 (1)	Rh-C(2)	2.021 (8)	P(2)-C(25)	1.835 (9)
Rh-Cl	2.570 (2)	P(1)-C(1)	1.820 (8)	P(2)-C(31)	1.838 (10)
Rh-Cl'	2.425 (2)	P(1)-C(7)	1.861 (10)	C(1)-C(2')	1.425 (14)
Rh-P(1)	2.234 (2)	P(1)-C(13)	1.824 (8)	C(1)-C(6)	1.396 (11)
Rh-P(2)	2.403 (2)	P(2)-C(19)	1.848 (8)	C(7)-C(12)	1.395 (13)
Bond Angles (deg)					
Rh'-Rh-Cl	57.14 (6)	Cl'-Rh-P(1)	153.78 (8)	Rh-P(2)-C(19)	118.3 (4)
Rh'-Rh-Cl'	62.92 (5)	Cl'-Rh-P(2)	96.63 (8)	C(19)-P(2)-C(25)	98.4 (4)
Rh'-Rh-P(1)	90.93 (6)	Cl'-Rh-C(2)	89.1 (3)	P(1)-C(1)-C(2')	120.1 (5)
Rh'-Rh-P(2)	152.40 (6)	P(1)-Rh-P(2)	108.67 (9)	C(2')-C(1)-C(6)	120.5 (7)
Rh'-Rh-C(2)	97.8 (3)	P(1)-Rh-C(2)	93.0 (2)	Rh-C(2)-C(1')	120.3 (6)
Cl-Rh-Cl'	80.81 (7)	P(2)-Rh-C(2)	100.3 (2)	P(1)-C(7)-C(12)	118.1 (7)
Cl-Rh-P(1)	86.48 (7)	Rh-Cl-Rh'	59.94 (5)	C(8)-C(7)-C(12)	123.0 (9)
Cl-Rh-P(2)	103.65 (7)	Rh-P(1)-C(1)	109.9 (3)	P(2)-C(19)-C(20)	120.8 (7)
Cl-Rh-C(2)	154.9 (3)	C(1)-P(1)-C(7)	104.3 (4)	C(20)-C(19)-C(24)	120.9 (8)

<sup>a</sup>Numbers in parentheses are estimated standard deviations in the least significant digits.

Table V. Selected Bond Distances and Bond Angles for  $\text{Rh}_2\text{Cl}_2(\text{Ph}_2\text{P}(\text{C}_6\text{H}_4))_2(\text{PMe}_3)_2$ 

Bond Distances (Å)					
Rh(1)-Rh(2)	2.506 (1)	Rh(2)-Cl(2)	2.503 (3)	P(3)-C(40)	1.850 (11)
Rh(1)-Cl(1)	2.529 (3)	Rh(2)-P(2)	2.224 (3)	P(3)-C(41)	1.823 (11)
Rh(1)-Cl(2)	2.506 (3)	Rh(2)-P(4)	2.348 (4)	P(3)-C(42)	1.855 (10)
Rh(1)-P(1)	2.220 (3)	Rh(2)-C(2)	1.991 (13)	C(1)-C(2)	1.41 (2)
Rh(1)-P(3)	2.363 (4)	P(1)-C(1)	1.815 (13)	C(1)-C(6)	1.44 (2)
Rh(1)-C(20)	2.023 (13)	P(1)-C(7)	1.828 (13)		
Rh(2)-Cl(1)	2.477 (3)	P(1)-C(13)	1.838 (13)		
Bond Angles (deg)					
Rh(2)-Rh(1)-Cl(1)	58.92 (8)	Cl(2)-Rh(1)-P(3)	106.1 (1)	Rh(1)-P(3)-C(40)	122.2 (4)
Rh(2)-Rh(1)-Cl(2)	59.92 (8)	Cl(2)-Rh(1)-C(20)	85.0 (4)	C(40)-P(3)-C(41)	99.7 (5)
Rh(2)-Rh(1)-P(1)	87.55 (9)	P(1)-Rh(1)-P(3)	105.8 (1)	P(1)-C(1)-C(2)	119.8 (9)
Rh(2)-Rh(1)-P(3)	156.2 (1)	P(1)-Rh(1)-C(20)	97.3 (4)	P(1)-C(1)-C(6)	118 (1)
Rh(2)-Rh(1)-C(20)	98.6 (4)	P(3)-Rh(1)-C(20)	99.1 (4)	C(2)-C(1)-C(6)	122 (1)
Cl(1)-Rh(1)-Cl(2)	78.1 (1)	Rh(1)-Rh(2)-Cl(1)	61.00 (8)	Rh(2)-C(2)-C(1)	118.4 (9)
Cl(1)-Rh(1)-P(1)	88.6 (1)	Cl(1)-Rh(2)-Cl(2)	79.1 (1)	Rh(1)-C(20)-C(19)	120.4 (9)
Cl(1)-Rh(1)-P(3)	101.0 (1)	Rh(1)-Cl(1)-Rh(2)	60.08 (8)	C(19)-C(20)-C(21)	116 (1)
Cl(1)-Rh(1)-C(20)	156.6 (4)	Rh(1)-P(1)-C(1)	111.5 (4)		
Cl(2)-Rh(1)-P(1)	147.3 (1)	C(1)-P(1)-C(7)	105.5 (6)		

<sup>a</sup>Numbers in parentheses are estimated standard deviations in the least significant digits.

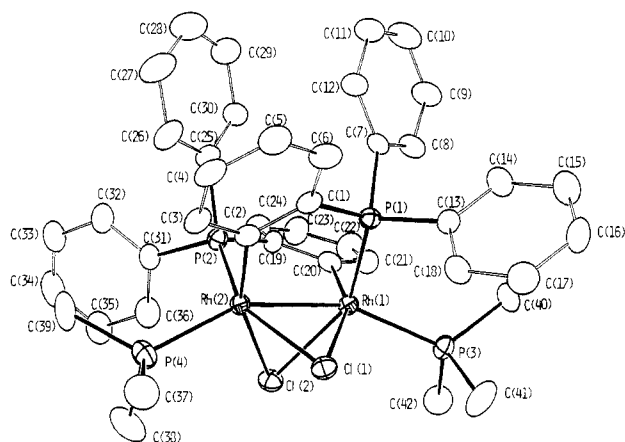


Figure 2. ORTEP drawing of the  $\text{Rh}_2(\mu\text{-Cl})_2(\text{C}_6\text{H}_4\text{PPh}_2)_2(\text{PMe}_3)_2$  molecule (**2**) showing the atom numbering. Each atom is represented by its ellipsoid of thermal displacement at the 30% probability level.

The C-Rh-Rh-P torsion angles are  $0.29^\circ$  in **1** and  $10.7^\circ$  in **2**.

Despite the moderate torsional twist in **2** it may still be said that both molecules consist of square pyramidally coordinated Rh atoms sharing a common basal edge (Cl...Cl) and having the monodentate phosphine atoms at the apex. The Rh-Rh-P angles are essentially the same (ca.  $153^\circ$ ) in the two molecules.

It is noteworthy that once again this type of structure, with two  $\mu\text{-Cl}$  groups, has been adopted. The possibility certainly exists, at least for the small  $\text{PMe}_3$  ligand, that two more phosphine ligands might have been incorporated so as to give a structure like that of  $\text{Rh}_2(\text{C}_6\text{H}_4\text{PPh}_2)_2(\text{dmpm})_2\text{Cl}_2$ . In this type of structure, as in

the one actually adopted, there would be a total of 10 metal-ligand bonds as well as a Rh-Rh bond. Evidently, the two types of structures do not differ greatly in stability and small, largely unpredictable factors can determine the preference in any given case.

**Acknowledgment.** We thank the National Science Foundation for support and Drs. Rinaldo Poli, Lee Daniels, and L. R. Falvello for crystallographic advice.

**Registry No.** **1**, 110745-24-9; **2**, 110745-26-1;  $\text{Rh}_2(\text{O}_2\text{CCH}_3)_2(\text{C}_6\text{H}_4\text{PPh}_2)_2$ , 92669-59-5; Rh, 7440-16-6;  $\text{Rh}_2\text{Cl}_2(\text{C}_6\text{H}_4\text{PPh}_2)_2(\text{PMe}_3)_2$ , 110745-25-0.

**Supplementary Material Available:** For the crystal structures of **1** and **2**, full tables of bond distances, bond angles, and anisotropic displacement parameters (15 pages); tables of observed and calculated structure factors (56 pages). Ordering information is given on any current masthead page.

Contribution from the Department of Chemistry and Laboratory for Molecular Structure and Bonding, Texas A&M University, College Station, Texas 77843

### Two Diastereomeric Forms of the Bichelated, Edge-Sharing Biocahedral Molecule $\text{Ta}_2\text{Cl}_6(\text{Et}_2\text{PCH}_2\text{CH}_2\text{PET}_2)_2$

F. Albert Cotton,\* Michael P. Diebold, and Wieslaw J. Roth

Received June 3, 1987

Chelate rings in metal complexes can often exist in more than one conformation. Five membered nonplanar rings such as those formed by chelating depe = bis(diethylphosphino)ethane

**Table I.** Crystallographic Data for Ta<sub>2</sub>Cl<sub>6</sub>(depe)<sub>2</sub>·C<sub>7</sub>H<sub>8</sub> (1) and Ta<sub>2</sub>Cl<sub>6</sub>(depe)<sub>2</sub> (2)

	Ta <sub>2</sub> Cl <sub>6</sub> P <sub>4</sub> C <sub>27</sub> H <sub>36</sub>	Ta <sub>2</sub> Cl <sub>6</sub> P <sub>4</sub> C <sub>20</sub> H <sub>48</sub>
formula	Ta <sub>2</sub> Cl <sub>6</sub> P <sub>4</sub> C <sub>27</sub> H <sub>36</sub>	Ta <sub>2</sub> Cl <sub>6</sub> P <sub>4</sub> C <sub>20</sub> H <sub>48</sub>
fw	1078.3	993.1
space group	P $\bar{1}$	Pca2 <sub>1</sub>
systematic absences		0kl, l ≠ 2n; h0l, h ≠ 2n
a, Å	10.291 (2)	14.854 (2)
b, Å	10.508 (2)	16.654 (3)
c, Å	10.108 (2)	13.631 (2)
α, deg	111.61 (2)	90.0
β, deg	93.51 (2)	90.0
γ, deg	98.48 (2)	90.0
V, Å <sup>3</sup>	995.9 (4)	3371.8 (7)
Z	1	4
d <sub>calcd</sub> , g/cm <sup>3</sup>	1.799	1.956
cryst size, mm	0.10 × 0.10 × 0.05	0.70 × 0.30 × 0.15
μ(Mo Kα), cm <sup>-1</sup>	60.103	70.906
data collect instrum	Rigaku AFC-5R	Syntex P3
radiation (monochromated in incident beam)	Mo Kα (λ <sub>K</sub> = 0.71073 Å)	
orientation reflns: no.; range (2θ), deg	20; 21.5–27.7	25; 17.9–29.2
temp, °C	21	21
scan method	θ–2θ	θ–2θ
data collect range, 2θ, deg	4 < 2θ < 45	4 < 2θ < 50
no. of unique data, total with F <sub>o</sub> <sup>2</sup> > 3σ(F <sub>o</sub> <sup>2</sup> )	2611, 2120	2262, 2112
no. of params refined	161	188
abs cor: max; min	1.00; 0.74	1.00; 0.73
R <sup>a</sup>	0.0370	0.0337
R <sub>w</sub> <sup>b</sup>	0.0500	0.0438
quality-of-fit indicator <sup>c</sup>	1.084	0.959
largest shift/esd, final cycle	0.26	0.01
largest peak, e/Å <sup>3</sup>	1.056	0.921

<sup>a</sup>R = Σ||F<sub>o</sub> - |F<sub>c</sub>|| / Σ|F<sub>o</sub>|. <sup>b</sup>R<sub>w</sub> = [Σw(|F<sub>o</sub> - |F<sub>c</sub>||)<sup>2</sup> / Σw|F<sub>o</sub>|<sup>2</sup>]<sup>1/2</sup>; w = 1/σ<sup>2</sup>(|F<sub>o</sub>|). <sup>c</sup>Quality of fit = [Σw(|F<sub>o</sub> - |F<sub>c</sub>||)<sup>2</sup> / (N<sub>observns</sub> - N<sub>params</sub>)]<sup>1/2</sup>.

are puckered, and two conformations, λ and δ, are possible.<sup>1</sup> When more than one ring is present in a molecule, diastereomeric isomerism is possible. For mononuclear complexes there can be significant differences in the relative stabilities between the diastereomers because of the different nonbonded (repulsive) interactions in each case. These different nonbonded interactions manifest themselves not only in relative stabilities but also in differences in M–L bond distances and L–M–L bond angles. For dinuclear complexes in which one chelate ring is bound to each metal atom, the differences in nonbonded interactions between the diastereomers is expected to be much less. This is especially true when the chelate rings are far enough apart to preclude direct steric interactions.

During our recent investigations of polynuclear low-valent complexes of niobium and tantalum<sup>2</sup> we have isolated and characterized two diastereomeric forms of Ta<sub>2</sub>Cl<sub>6</sub>(depe)<sub>2</sub>. While these diastereomers differ in ring conformation, there is virtually no difference in intramolecular distances and angles. The absence of such effects is of significance with respect to our understanding of some other compounds that we shall report later.

### Experimental Section

**Synthesis.** All manipulations were performed under an atmosphere of argon with use of standard Schlenk line techniques. Solvents were freshly distilled prior to use. P-*n*-Bu<sub>3</sub> was purchased from Aldrich Chemical Co. and used as received. Ta<sub>2</sub>Cl<sub>6</sub>(μ-THT)(THF)<sub>2</sub> was prepared by dissolving Ta<sub>2</sub>Cl<sub>6</sub>(THT)<sub>3</sub><sup>3</sup> and collecting the precipitate that formed after 1 day.

**Table II.** Positional and Isotropic-Equivalent Displacement Parameters for Ta<sub>2</sub>Cl<sub>6</sub>(depe)<sub>2</sub>·C<sub>7</sub>H<sub>8</sub> (1)<sup>a</sup>

atom	x	y	z	B, Å <sup>2</sup>
Ta	-0.08631 (4)	0.06341 (4)	0.08725 (4)	3.296 (9)
Cl(1)	-0.0487 (3)	-0.1708 (3)	0.0483 (3)	4.35 (6)
Cl(2)	-0.2817 (3)	-0.0131 (3)	-0.0856 (3)	4.70 (7)
Cl(3)	0.0660 (3)	0.1693 (3)	0.3047 (3)	5.03 (7)
P(1)	-0.2586 (3)	0.0196 (3)	0.2547 (3)	4.25 (7)
P(2)	-0.1597 (3)	0.3033 (3)	0.1866 (3)	4.33 (7)
C(1)	-0.340 (1)	0.170 (1)	0.307 (1)	5.9 (3)
C(2)	-0.243 (1)	0.307 (1)	0.344 (1)	5.7 (3)
C(11)	-0.190 (1)	0.007 (1)	0.423 (1)	5.5 (3)
C(12)	-0.284 (2)	0.018 (2)	0.534 (1)	8.8 (5)
C(13)	-0.404 (1)	-0.122 (1)	0.181 (1)	5.7 (3)
C(14)	-0.370 (1)	-0.266 (1)	0.132 (2)	7.7 (4)
C(21)	-0.026 (1)	0.461 (1)	0.258 (1)	6.3 (4)
C(22)	-0.067 (2)	0.599 (2)	0.316 (2)	9.1 (5)
C(23)	-0.282 (1)	0.343 (1)	0.078 (1)	5.7 (3)
C(24)	-0.226 (2)	0.360 (2)	-0.054 (1)	7.8 (4)
C(s1)	0.426 (2)	0.380 (2)	0.469 (2)	8.9 (4)*
C(s2)	0.379 (4)	0.453 (4)	0.275 (4)	9.3 (9)*
C(s3)	0.492 (3)	0.409 (3)	0.586 (3)	13.8 (8)*
C(s4)	0.413 (2)	0.439 (2)	0.368 (2)	12.8 (7)*

<sup>a</sup>Starred values are for atoms refined isotropically. Anisotropically refined atoms are given in the form of the equivalent isotropic displacement parameter defined as  $\frac{1}{3}[a^2\beta_{11} + b^2\beta_{22} + c^2\beta_{33} + ab(\cos \gamma)\beta_{12} + ac(\cos \beta)\beta_{13} + bc(\cos \alpha)\beta_{23}]$ .

To a slurry of 0.42 g (0.50 mmol) of Ta<sub>2</sub>Cl<sub>6</sub>(μ-THT)(THF)<sub>2</sub> in 10 mL of toluene and 0.5 mL (2.0 mmol) of P-*n*-Bu<sub>3</sub> was added sodium amalgam (1.0 mmol of Na in 0.5 mL of Hg). After it was stirred for 3 h, the red solution was filtered and layered with a solution of 0.1 mL of depe in 20 mL of hexane. Crystals grew after several days. Crystals of two habits could be distinguished under the microscope, and subsequent crystallographic analysis revealed that they had different unit cell parameters. One crystal of each type was subjected to a complete crystal structure determination.

**X-ray Crystallography.** X-ray structure determinations were carried out by application of procedures routine to this laboratory and detailed elsewhere.<sup>4,5</sup> Relevant crystallographic data for both compounds are summarized in Table I. For each compound polarization, Lorentz, and absorption corrections were applied to the data. The last corrections were based on azimuthal (ψ) scans of nine reflections with Eulerian angle χ near 90°.

The location of the metal atom in **1** was derived from a three-dimensional Patterson function. Space group P $\bar{1}$  was assumed from the outset, and the remainder of the non-hydrogen atoms were located during a series of least-squares refinements and difference Fourier syntheses. A disordered molecule of toluene was located about an inversion center and was refined with isotropic displacement parameters. All other atoms were assigned anisotropic displacement parameters, and the structure was refined to convergence. A few peaks of intensity near 1.0 e/Å<sup>3</sup> were present in the final difference Fourier map but were located close to the heavy atoms.

Systematic absences revealed two possible space groups for **2**. The structure could be developed only in the noncentrosymmetric one, viz., Pca2<sub>1</sub>. The metal atom positions were determined from a three-dimensional Patterson function, and the remaining non-hydrogen atoms were located during a series of least-squares refinements and difference Fourier syntheses. All atoms were given anisotropic displacement parameters, and the structure was refined to convergence. Refinement of the enantiomorph indicated that the initial choice was correct. Because of the polar nature of this molecule (vide infra) refinement in the centrosymmetric space group Pcam was not possible without inclusion of disorder.

Tables of observed and calculated structure factors and anisotropic displacement parameters for both compounds are available as supplementary material.

### Results and Discussion

**Synthesis.** The intended purpose of this research was the synthesis of Ta<sub>3</sub>Cl<sub>7</sub>(depe)<sub>3</sub> via the reduction of Ta<sub>2</sub>Cl<sub>6</sub>(μ-THT)(THF)<sub>2</sub> to Ta<sub>3</sub>Cl<sub>7</sub>(P-*n*-Bu<sub>3</sub>)<sub>6</sub> and subsequent reaction with

- Hawkins, C. J. *Absolute Configuration of Metal Complexes*; Wiley-Interscience: New York, 1971.
- (a) Cotton, F. A.; Diebold, M. P.; Roth, W. J. *J. Am. Chem. Soc.* **1986**, *108*, 3538. (b) Cotton, F. A.; Diebold, M. P.; Roth, W. J. *J. Am. Chem. Soc.* **1987**, *109*, 2833. (c) Cotton, F. A.; Diebold, M. P.; Roth, W. J. *J. Am. Chem. Soc.* **1987**, *109*, 5506.
- Templeton, J. L.; McCarley, R. E. *Inorg. Chem.* **1978**, *17*, 2293.

- Bino, A.; Cotton, F. A.; Fanwick, P. E. *Inorg. Chem.* **1979**, *18*, 3558.
- Calculations were done on a departmental VAX 11-780 computer with SDP programming software.

**Table III.** Positional Parameters and Their Estimated Standard Deviations for Ta<sub>2</sub>Cl<sub>6</sub>(depe)<sub>2</sub> (2)<sup>a</sup>

atom	x	y	z	B, Å <sup>2</sup>
Ta(1)	0.08643 (4)	0.22125 (4)	0.000	2.70 (1)
Ta(2)	-0.05065 (4)	0.28835 (4)	0.10624 (7)	2.65 (1)
Cl(1)	-0.0662 (3)	0.1661 (3)	0.0104 (4)	3.45 (8)
Cl(2)	0.1016 (3)	0.3426 (3)	0.1001 (4)	3.96 (9)
Cl(3)	0.1431 (3)	0.1322 (3)	0.1258 (3)	4.1 (1)
Cl(4)	0.0604 (3)	0.2900 (3)	-0.1516 (3)	4.1 (1)
Cl(5)	-0.0234 (3)	0.2161 (3)	0.2581 (3)	3.91 (9)
Cl(6)	-0.1113 (3)	0.3753 (3)	-0.0181 (3)	4.1 (1)
P(1)	0.1231 (3)	0.0972 (3)	-0.1112 (4)	3.7 (1)
P(2)	0.2578 (3)	0.2437 (3)	-0.0346 (4)	4.0 (1)
P(3)	-0.0868 (3)	0.4119 (3)	0.2201 (4)	3.5 (1)
P(4)	-0.2186 (3)	0.2609 (3)	0.1537 (4)	3.4 (1)
C(1)	0.242 (2)	0.102 (1)	-0.145 (2)	7.9 (6)*
C(2)	0.302 (2)	0.148 (2)	-0.081 (3)	11 (1)*
C(3)	-0.212 (1)	0.417 (1)	0.226 (2)	4.8 (4)*
C(4)	-0.252 (2)	0.334 (1)	0.254 (2)	4.6 (4)*
C(11)	0.120 (2)	-0.002 (2)	-0.059 (2)	7.3 (6)*
C(12)	0.014 (3)	-0.030 (2)	-0.052 (3)	11 (1)*
C(13)	0.065 (2)	0.094 (2)	-0.229 (2)	7.4 (7)*
C(14)	0.101 (2)	0.025 (2)	-0.299 (2)	9.8 (9)*
C(21)	0.296 (2)	0.315 (2)	-0.123 (2)	8.2 (7)*
C(22)	0.290 (2)	0.401 (2)	-0.078 (3)	11 (1)*
C(23)	0.333 (2)	0.256 (1)	0.073 (2)	5.4 (5)*
C(24)	0.433 (2)	0.258 (2)	0.051 (2)	6.4 (6)*
C(31)	-0.048 (1)	0.407 (1)	0.349 (1)	4.1 (4)*
C(32)	-0.087 (1)	0.468 (1)	0.421 (2)	5.9 (5)*
C(33)	-0.060 (1)	0.516 (1)	0.183 (1)	4.4 (4)*
C(34)	0.040 (1)	0.537 (1)	0.200 (2)	5.3 (5)*
C(41)	-0.242 (1)	0.160 (1)	0.208 (2)	4.7 (4)*
C(42)	-0.338 (2)	0.146 (1)	0.246 (2)	6.3 (5)*
C(43)	-0.305 (1)	0.276 (1)	0.064 (1)	4.3 (4)*
C(44)	-0.307 (2)	0.210 (1)	-0.016 (2)	6.3 (6)*

<sup>a</sup>See footnote a for Table II.**Table IV.** Important Bond Distances and Angles in Ta<sub>2</sub>Cl<sub>6</sub>(depe)<sub>2</sub>-C<sub>7</sub>H<sub>8</sub> (1)<sup>a</sup>

A. Distances (Å)			
Ta-Ta'	2.724 (1)	Ta-Cl(3)	2.402 (3)
Ta-Cl(1)	2.441 (3)	Ta-P(1)	2.629 (3)
Ta-Cl(1)'	2.444 (3)	Ta-P(2)	2.597 (3)
Ta-Cl(2)	2.404 (3)		
B. Angles (deg)			
Ta'-Ta-Cl(1)	56.15 (7)	Cl(1)'-Ta-Cl(2)	94.8 (1)
Ta'-Ta-Cl(1)'	56.06 (7)	Cl(1)'-Ta-Cl(3)	94.9 (1)
Ta'-Ta-Cl(2)	98.94 (6)	Cl(1)'-Ta-P(1)	162.4 (1)
Ta'-Ta-Cl(3)	97.26 (7)	Cl(1)'-Ta-P(2)	83.5 (1)
Ta'-Ta-P(1)	141.47 (7)	Cl(2)-Ta-Cl(3)	163.8 (1)
Ta'-Ta-P(2)	139.42 (8)	Cl(2)-Ta-P(1)	82.36 (9)
Cl(1)-Ta-Cl(1)'	112.21 (9)	Cl(2)-Ta-P(2)	86.48 (9)
Cl(1)-Ta-Cl(2)	95.2 (1)	Cl(3)-Ta-P(1)	84.55 (9)
Cl(1)-Ta-Cl(3)	93.2 (1)	Cl(3)-Ta-P(2)	81.7 (1)
Cl(1)-Ta-P(1)	85.3 (1)	P(1)-Ta-P(2)	79.0 (1)
Cl(1)-Ta-P(2)	163.9 (1)	Ta-Cl(1)-Ta'	67.79 (8)

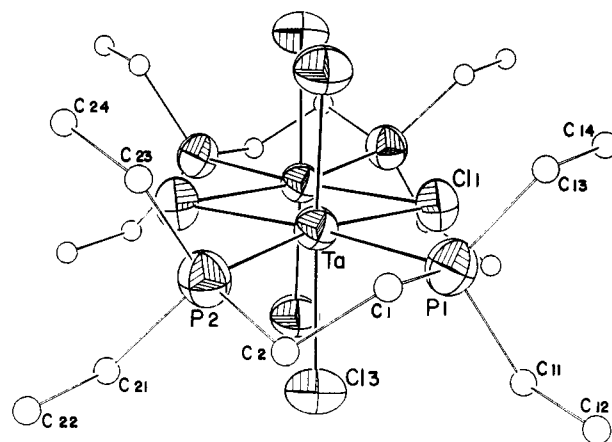
<sup>a</sup>Numbers in parentheses are estimated deviations in the least significant digit.

depe. A similar reaction sequence had been used to prepare Nb<sub>3</sub>Cl<sub>7</sub>(dmpe)<sub>3</sub>.<sup>2b</sup> Instead, Ta<sub>2</sub>Cl<sub>6</sub>(depe)<sub>2</sub> was the only product isolated. This compound is undoubtedly the product of the reaction of depe with an unreduced tantalum species (probably Ta<sub>2</sub>Cl<sub>6</sub>-(μ-THT)(P-*n*-Bu<sub>3</sub>)<sub>2</sub>). While no attempt has been made to prepare this complex in a more direct manner, this could most likely be done by the straightforward reaction of depe with Ta<sub>2</sub>Cl<sub>6</sub>L<sub>3</sub> (L = THT, SME<sub>2</sub>), as for the case of the homologue Nb<sub>2</sub>Cl<sub>6</sub>(depe)<sub>2</sub>, which is obtained from Nb<sub>2</sub>Cl<sub>6</sub>(SME<sub>2</sub>)<sub>3</sub>.<sup>6</sup>

**Structure.** Atomic positional and isotropic-equivalent displacement parameters for structures **1** and **2** are given in Tables II and III, respectively. Important bond distances and angles are presented in Table IV for **1** and Table V for **2**.

**Table V.** Important Bond Distances and Angles in Ta<sub>2</sub>Cl<sub>6</sub>(depe)<sub>2</sub> (2)<sup>a</sup>

(A) Distances (Å)			
Ta(1)-Ta(2)	2.737 (1)	Ta(2)-Cl(1)	2.429 (5)
Ta(1)-Cl(1)	2.450 (4)	Ta(2)-Cl(2)	2.437 (5)
Ta(1)-Cl(2)	2.449 (5)	Ta(2)-Cl(5)	2.428 (5)
Ta(1)-Cl(3)	2.418 (5)	Ta(2)-Cl(6)	2.405 (5)
Ta(1)-Cl(4)	2.393 (5)	Ta(2)-P(3)	2.632 (5)
Ta(1)-P(1)	2.620 (6)	Ta(2)-P(4)	2.618 (5)
Ta(1)-P(2)	2.616 (5)		
(B) Angles (deg)			
Ta(2)-Ta(1)-Cl(1)	55.5 (1)	Ta(1)-Ta(2)-Cl(1)	56.2 (1)
Ta(2)-Ta(1)-Cl(2)	55.7 (1)	Ta(1)-Ta(2)-Cl(2)	56.1 (1)
Ta(2)-Ta(1)-Cl(3)	97.7 (1)	Ta(1)-Ta(2)-Cl(5)	97.2 (1)
Ta(2)-Ta(1)-Cl(4)	98.1 (1)	Ta(1)-Ta(2)-Cl(6)	98.7 (1)
Ta(2)-Ta(1)-P(1)	141.5 (1)	Ta(1)-Ta(2)-P(3)	141.5 (1)
Ta(2)-Ta(1)-P(2)	139.6 (1)	Ta(1)-Ta(2)-P(4)	140.2 (1)
Cl(1)-Ta(1)-Cl(2)	111.2 (2)	Cl(1)-Ta(2)-Cl(2)	112.3 (2)
Cl(1)-Ta(1)-Cl(3)	92.9 (2)	Cl(1)-Ta(2)-Cl(5)	93.4 (2)
Cl(1)-Ta(1)-Cl(4)	94.6 (2)	Cl(1)-Ta(2)-Cl(6)	95.2 (2)
Cl(1)-Ta(1)-P(1)	86.0 (2)	Cl(1)-Ta(2)-P(3)	162.3 (2)
Cl(1)-Ta(1)-P(2)	164.7 (2)	Cl(1)-Ta(2)-P(4)	84.0 (2)
Cl(2)-Ta(1)-Cl(3)	94.5 (2)	Cl(2)-Ta(2)-Cl(5)	93.3 (2)
Cl(2)-Ta(1)-Cl(4)	95.8 (2)	Cl(2)-Ta(2)-Cl(6)	95.7 (2)
Cl(2)-Ta(1)-P(1)	162.5 (2)	Cl(2)-Ta(2)-P(3)	85.4 (2)
Cl(2)-Ta(1)-P(2)	83.9 (2)	Cl(2)-Ta(2)-P(4)	163.3 (2)
Cl(3)-Ta(1)-Cl(4)	164.1 (2)	Cl(5)-Ta(2)-Cl(6)	164.1 (2)
Cl(3)-Ta(1)-P(1)	81.6 (2)	Cl(5)-Ta(2)-P(3)	85.3 (2)
Cl(3)-Ta(1)-P(2)	82.9 (2)	Cl(5)-Ta(2)-P(4)	82.0 (2)
Cl(4)-Ta(1)-P(1)	84.9 (2)	Cl(6)-Ta(2)-P(3)	82.4 (2)
Cl(4)-Ta(1)-P(2)	86.2 (2)	Cl(6)-Ta(2)-P(4)	85.5 (2)
P(1)-Ta(1)-P(2)	78.8 (2)	P(3)-Ta(2)-P(4)	78.3 (2)
		Ta(1)-Cl(1)-Ta(2)	68.3 (1)
		Ta(1)-Cl(2)-Ta(2)	68.1 (1)

<sup>a</sup>Numbers in parentheses are estimated deviations in the least significant digit.**Figure 1.** ORTEP view and atom-labeling scheme for Ta<sub>2</sub>Cl<sub>6</sub>(depe)<sub>2</sub>-C<sub>7</sub>H<sub>8</sub> (1). Carbon atoms are drawn as spheres of arbitrary diameter.

Two distinct crystalline forms of Ta<sub>2</sub>Cl<sub>6</sub>(depe)<sub>2</sub> were isolated. They could be distinguished optically and were revealed by X-ray crystallographic analysis to be diastereomers of one another. The difference between these molecules is in the conformations of the five-membered M-P-C-C-P rings. Form **1** is the meso compound; one ring is λ while the other is δ. This molecule is achiral and has virtual C<sub>2h</sub> symmetry, the twofold axis passing along the metal-metal vector (see Figure 1). Form **2** is chiral; both rings have the λ configuration (see Figure 2). This compound has virtual D<sub>2</sub> symmetry, the twofold axes intersecting at the midpoint of the Ta-Ta bond. This latter form of Ta<sub>2</sub>Cl<sub>6</sub>(depe)<sub>2</sub> is isomorphous with the subsequently characterized Nb<sub>2</sub>Cl<sub>6</sub>(depe)<sub>2</sub>.<sup>6</sup>

There are no significant differences in intramolecular dimensions between the two forms (see Tables IV and V). This is not surprising as the large distance between the five-membered rings would tend to minimize the differences in steric repulsion between the diastereomers. All metal-ligand distances are normal, and

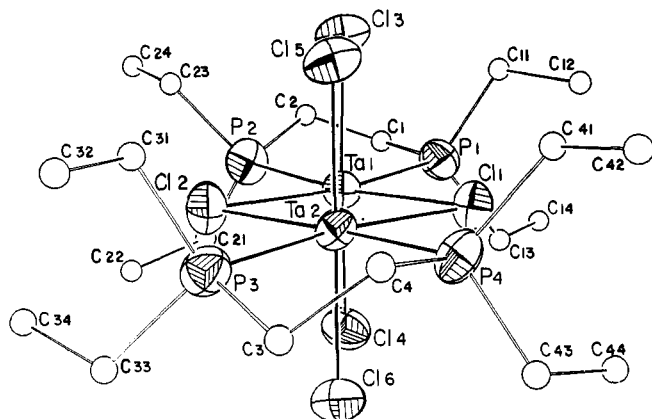


**Figure 2.** ORTEP view and atom-labeling scheme for  $\text{Ta}_2\text{Cl}_6(\text{depe})_2$  (**2**). Carbon atoms are drawn as spheres of arbitrary diameter.

the metal-metal distances indicate the presence of Ta-Ta double bonds, which would be expected between the two  $d^2$  metal atoms.

**Acknowledgment.** We are grateful to the National Science Foundation for support. M.P.D. thanks the National Science Foundation for a NSF Predoctoral Fellowship and Texaco/IUCCP for additional support.

**Registry No.** 1, 110796-21-9; 2, 110796-20-8; Ta, 7440-25-7.

**Supplementary Material Available:** Complete tables of bond distances and angles and tables of anisotropic displacement parameters for both compounds (6 pages); tables of calculated and observed structure factors for both compounds (22 pages). Ordering information is given on any current masthead page.

Contribution from the Department of Chemistry and Lawrence Berkeley Laboratory, University of California, Berkeley, California 94720, and Department of Chemistry, University of the Pacific, Stockton, California 95211

### Temperature-Dependent Valence Isomerization in a Manganese Tetraphenylporphyrin

Anthony C. Maliyackel, J. W. Otvos, Melvin Calvin, and L. O. Spreer\*

Received May 7, 1987

The characterization of oxidized metalloporphyrins is of much current interest because they serve as model systems for many redox reactions of metalloporphyrin-containing enzymes. It is well-established that oxidation of a metalloporphyrin can be metal-centered or ligand-centered, the latter producing a  $\pi$  cation radical. Our interest in this subject, particularly in the characterization of high-valent manganese porphyrins, derives from our work on potential multipole-electron redox catalysts for an artificial photosynthesis assembly.<sup>1</sup> A prerequisite for a multiple-electron redox catalyst is the accessibility of a variety of oxidation states. Manganese porphyrins have been fully characterized with manganese in the +2, +3,<sup>2</sup> +4,<sup>3,4</sup> and +5<sup>5</sup> oxidation states. In addition, several groups have described manganese  $\pi$ -cation-radical porphyrins<sup>6,7</sup> where oxidation has occurred on the macrocycle.

The axial ligands on the metal are of prime importance in determining the electronic configuration of oxidized metalloporphyrins. Recently we described a case in which a Mn(III) tetraphenylporphyrin  $\pi$  cation radical,  $\text{Mn}^{\text{III}}\text{TPP}^{\pi+}$ , is converted to a  $\text{Mn}^{\text{IV}}\text{TPP}$  species by addition of a strong  $\pi$ -donating ligand,  $\text{CH}_3\text{O}^-$ .<sup>8</sup> In the present paper we describe the preparation and

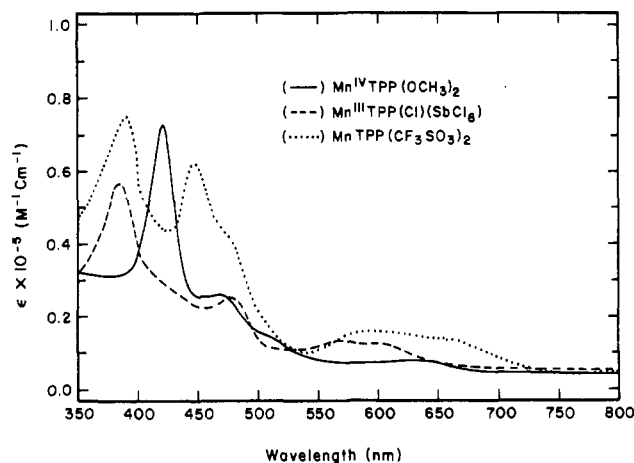


**Figure 1.** Electronic spectra of manganese tetraphenylporphyrin species: (—)  $\text{Mn}^{\text{IV}}\text{TPP}(\text{OCH}_3)_2$ ; (---)  $\text{Mn}^{\text{III}}\text{TPP}(\text{Cl})(\text{SbCl}_6)$  ( $\text{Mn}^{\text{III}}$   $\pi$  cation radical); (····)  $\text{MnTPP}(\text{CF}_3\text{SO}_3)_2$ .

properties of the compound  $\text{MnTPP}(\text{CF}_3\text{SO}_3)_2$ , which we believe undergoes a temperature-dependent valence isomerization from a manganese(III)  $\pi$  cation radical at higher temperature to a manganese(IV) porphyrin at reduced temperatures.

### Experimental Section

The chemicals used were all reagent grade. Dichloromethane and toluene were purified by distillation and stored over activated molecular sieves. Preparation of  $\text{Mn}^{\text{III}}\text{TPP}(\text{Cl})$  is discussed elsewhere.<sup>8</sup>

**Synthesis of  $\text{MnTPP}(\text{CF}_3\text{SO}_3)_2$ .** To a solution of  $\text{Mn}^{\text{III}}\text{TPP}(\text{Cl})$  (0.5 mM) in dichloromethane (50 mL) at  $-70^\circ\text{C}$  were added solutions of iodine (2.0 mM) in dichloromethane (15 mL) and silver trifluoromethane sulfonate (1.0 mM) in toluene (10 mL). After the mixture was stirred for 15 min, the precipitate of silver iodide and silver chloride was filtered off quickly. The filtrate was then added to an excess of hexane kept at  $-70^\circ\text{C}$ . The resulting precipitate was collected by filtration and air-dried. Anal. Calcd for  $\text{MnTPP}(\text{CF}_3\text{SO}_3)_2$ : Mn, 5.69; C, 57.20; N, 5.80; H, 2.90; S, 6.63. Found: Mn, 5.41; C, 54.30; N, 5.31; H, 2.97; S, 6.28. (The experimental values are low compared to the calculated ones, but the experimental N/Mn mole ratio is 4.0 and the experimental S/Mn mole ratio is 2.0. Contamination by a small amount of moisture would account for the discrepancies.) The compound was free from Ag, I, and Cl (<0.5%).

Visible absorption spectra were recorded on a Hewlett-Packard 845A spectrometer. Variable-temperature magnetic susceptibility measurements in the solid state were carried out on a SQUID apparatus (SHE Corp., VPS 800 susceptometer). The experimental details are discussed elsewhere.<sup>8</sup> The X-band EPR spectra were recorded on a Varian Model E-109 spectrometer equipped with a low-temperature Dewar (Air Products, Ltd.).

### Results and Discussion

The compound  $\text{MnTPP}(\text{CF}_3\text{SO}_3)_2$  (**1**) is produced by a one-electron oxidation from the starting  $\text{Mn}^{\text{III}}\text{TPP}(\text{Cl})$  material. The oxidation could conceivably take place at the metal, producing a  $\text{Mn}^{\text{IV}}\text{TPP}^{2+}$  ion, or at the porphyrin ring, producing a Mn(III)  $\pi$ -cation-radical species. In fact, the electronic spectrum and solid-state magnetic susceptibility data, both near room temperature, support designation of **1** as a Mn(III)  $\pi$  cation radical. However, the magnetic moment of **1** shows a significant temperature dependence, and this, coupled with the features of the low-temperature (<80 K) EPR spectrum, strongly suggests that a temperature-dependent oxidation-state change takes place. At the lower temperatures the ground-state electronic configuration

- (1) Maliyackel, A. C.; Otvos, J. W.; Spreer, L. O.; Calvin, M. *Proc. Natl. Acad. Sci. U.S.A.* **1986**, *83*, 3572-3574.
- (2) Smith, D. M. *Porphyrins and Metalloporphyrins*; Elsevier: New York, 1975; pp 352-359.
- (3) Hill, C. L.; Schardt, B. C. *J. Am. Chem. Soc.* **1980**, *102*, 6374-6375.
- (4) Smegal, J. A.; Hill, C. L. *J. Am. Chem. Soc.* **1983**, *105*, 2920-2922.
- (5) Hill, C. L.; Hollander, F. J. *J. Am. Chem. Soc.* **1982**, *104*, 7318-7319.
- (6) Morehouse, K. M.; Neta, P. *J. Phys. Chem.* **1984**, *88*, 1575-1579.
- (7) Goff, H. M.; Phillippi, M. A.; Boersma, A. D.; Hansen, A. P. *Adv. Chem. Ser.* **1982**, No. 201, 357-376.
- (8) Spreer, L. O.; Maliyackel, A. C.; Holbrook, S.; Otvos, J. W.; Calvin, M. *J. Am. Chem. Soc.* **1986**, *108*, 1949-1953.

\* To whom correspondence should be addressed at the University of the Pacific.